

## Investigating Effects of Alloy Chemical Complexity on Helium Bubble Formation by Accurate Segregation Measurements Using Atom Probe Tomography

Xing Wang<sup>1</sup>, Ke Jin<sup>2</sup>, Di Chen<sup>3</sup>, Hongbin Bei<sup>2</sup>, Yongqiang Wang<sup>3</sup>, William J. Weber<sup>4,2</sup>, Yanwen Zhang<sup>2,4</sup>, Jonathan Poplawsky<sup>1</sup>, and Karren L. More<sup>1,\*</sup>

<sup>1</sup>. Center for Nanophase Materials Sciences, Oak Ridge National Laboratory, TN, USA.

<sup>2</sup>. Materials Science & Technology Division, Oak Ridge National Laboratory, TN, USA.

<sup>3</sup>. Materials Science & Technology Division, Los Alamos National Laboratory, NM, USA

<sup>4</sup>. Department of Materials Sciences, University of Tennessee-Knoxville, TN, USA.

\* Corresponding author: [morekl1@ornl.gov](mailto:morekl1@ornl.gov)

Due to its low solubility, He tends to cluster with vacancies to form bubbles in irradiated materials [1]. Previous studies showed that tuning the alloy chemical complexity in concentrated solid-solution alloys (CSAs) can be an effective approach to tailor defect energy landscapes and suppress He bubble growth [1,2]. In CSAs, multiple elements are randomly arranged in simple lattice structures, which generate extreme chemical complexity at the unit-cell level. A comprehensive understanding of how such chemical complexity affects defect generation and migration during irradiation is required. Here, atom probe tomography (APT) is used to accurately measure radiation-induced segregation near He bubbles, providing insight of defect energetics in CSAs.

Four CSAs (NiFe, NiCo, NiCoCr, and NiCoFe) and Ni were irradiated by 200 keV He ions at 500°C to a fluence of  $5 \times 10^{16}$  He/cm<sup>2</sup>. The size distributions of He bubbles were characterized using transmission electron microscopy (TEM). Field evaporation for APT was conducted in laser mode at 45 K with a pulse repetition rate of 200 kHz, a detection rate of 0.004 atoms per pulse, and a 70 pJ laser energy, such that more than twenty million ions were acquired from each sample for compositional analyses. A correlated TEM-APT study showed that He bubbles appeared as high-density regions in the APT reconstructions [3], so iso-density surfaces were used to locate the bubble positions in the APT reconstructions and elemental segregation to the bubble shell was measured using one-dimensional concentration profiles along the long axis of the needle.

TEM analyses show that growth of He bubbles is suppressed by increasing the alloy chemical complexity in CSAs. Fig. 1a compares He bubble size distributions in the five materials based on statistical analyses of regions between the irradiated surface and 350 nm below the surface. The resistance to He bubble growth follows as NiCoFe > NiFe > NiCoCr > NiCo, with Ni showing the lowest resistance. In general, the alloy becomes more resistant to He bubble growth as its chemical complexity increases. The interesting exception is NiCoCr, which exhibits a lower resistance to bubble growth than the binary NiFe and ternary NiCoFe. To understand this unexpected trend, the elemental segregation behavior near bubbles of similar sizes (~7 nm diameter) were measured using APT (Fig. 1b) and compared for the different CSAs. As shown in Fig. 2, Cr- and Fe-depletion and Ni- and Co-enrichment near the bubbles is typically observed, indicating vacancies diffuse primarily via Cr and Fe lattice sites, while interstitials diffuse via Ni and Co sites. More importantly, the magnitude of the Cr-depletion around the bubbles in NiCoCr is larger than that of Fe in NiCoFe, in which the Cr-content near bubbles in NiCoCr is as low as 5 at.%, while the Fe content near bubbles in NiCoFe is ~10 at.%. Because vacancy migration plays a dominant role in

bubble growth [2], a larger depletion of an element indicates a higher vacancy mobility for that element. Thus, the segregation measurements show that in Ni-based CSAs, vacancies diffuse much faster via Cr than via Fe, leading to faster vacancy clustering and a higher bubble growth rate in NiCoCr than NiCoFe. In NiCo, only a small amount of Co-depletion is observed near the bubble, suggesting that vacancies cannot diffuse fast enough via Co to suppress the generation of defects. Therefore, NiCo exhibits a lower resistance to bubble growth compared to other CSAs. These conclusions are supported by defect migration barriers determined from density functional theory calculations [4].

### References:

- [1] Z Fan, et al., *Acta. Mater.* **164** (2019), p. 283.
- [2] X Wang, et al., *Materialia* **5** (2019), p. 100183.
- [3] J Poplawsky, et al., *M&M 2019 Conference Proceedings* (2019).
- [4] S Zhao, et al., *Phys. Rev. Mater.* **2** (2018), p. 013602.
- [5] This work was supported as part of the Energy Dissipation to Defect Evolution (EDDE), an Energy Frontier Research Center funded by the U.S. Department of Energy (DOE), Office of Science, Basic Energy Sciences under contract number DE-AC05-00OR22725. Microscopy was performed as part of a user project at ORNL's Center for Nanophase Materials Sciences, which is a U.S. DOE, Office of Science User Facility. Helium implantations were supported by the Center for Integrated Nanotechnologies, which is a U.S. DOE Office of Science user facility jointly operated by Los Alamos and Sandia National Laboratories.

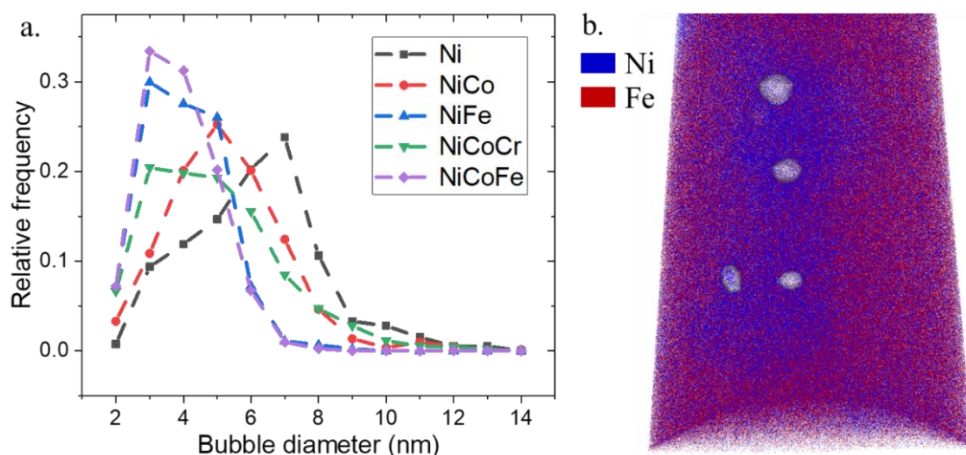


**Figure 1.** (a) Comparison of He bubble size distributions in Ni and Ni-based CSAs. (b) APT reconstruction of NiFe sample containing He bubbles (in white) and Fe-depleted zones around bubbles.

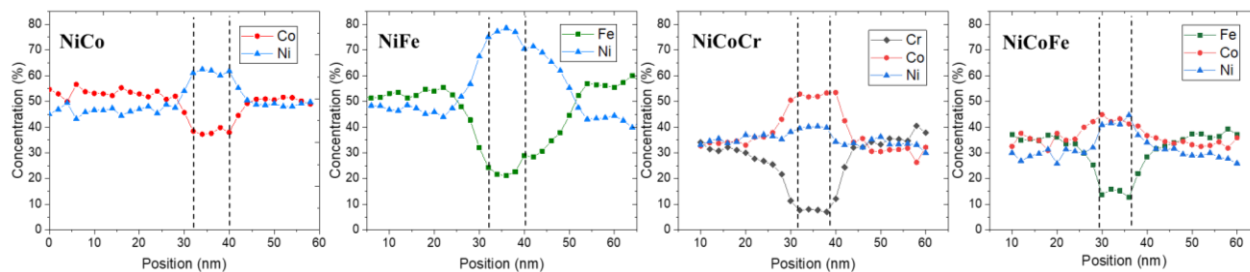


**Figure 2.** One-dimensional elemental concentration profiles across He bubbles in Ni-based CSAs. Position of He bubble is marked by two dashed vertical lines in each profile.